Indian Journal of Chemical Technology
Vol. 20, January 2013, pp. 15-20

Alumina-carbon composite as an effective adsorbent for removal of Methylene Blue and Alizarin Red-s from aqueous solution

Pranay A Raut, Monal Dutta, Sonali Sengupta & Jayanta Kumar Basu*
Indian Institute of Technology, Kharagpur, Kharagpur 721 302, India

Received 12 July 2011; accepted 30 August 2012

An alumina-carbon composite has been prepared by *in situ* precipitation of aluminium hydroxide on the surface of commercial activated carbon followed by calcinations. The adsorption characteristics of the as-synthesized material are studied using Methylene Blue and Alizarin Red-s. The adsorption equilibrium for Methylene Blue and Alizarin Red-s are well represented by the Redlich-Peterson and Tempkin isotherms respectively. The maximum adsorption capacity for Methylene Blue is found to be 1152.30 mg/g at *p*H 8 and that for Alizarin Red-s is 522.81 mg/g at *p*H 5. The adsorption kinetics for both the dyes has been explained by the pseudo-second-order model.

Keywords: Adsorption isotherm, Alizarin Red-S, Alumina-carbon composite, Methylene Blue

In the present decade the contamination of water bodies by colored effluents has become a serious concern. The textile, paper and plastic industries produce a vast amount of dyes every year and a significant amount of these dyes are directly discharged into water bodies. The dye compounds cause serious harm to aquatic life[1] and most of the dyes have complex aromatic structure and are difficult to biodegrade[2]. Among the various traditional water treatment methods for dye removal from waste water, such as adsorption, ion exchange, reverse osmosis, ultra filtration and chemical degradation etc[3,4], adsorption is a very popular and widely applied technique for removing non-biodegradable dyes[5-7]. There are many adsorbents available commercially such as activated carbon, bentonite, sepiolite, zeolite, kaolin, etc. Activated carbon shows the good adsorption characteristics towards non-polar pollutants and acidic dyes because of its large surface area and micro-porous nature. The bentonite, kaolin and zeolite show good adsorption capacity for congo red[8] and sepiolite shows good adsorption capacity for azo dyes[9,10] because of its silica tetrahedral structure[11-13]. On the other hand, activated alumina exhibits good adsorption capacity for basic dye malachite green[14] and the surfactant-modified alumina is used for the removal of crystal violet from water[15]. But the widespread use of activated carbon is restricted due to its high cost[16-19]. Activated carbon-sepiolite composite pellets have been prepared for both gas and liquid phase application[20]. Keoline-carbon composite has been used as an adsorbent for carotene removal from red palm oil[21]. Carbon nanotube-alumina composite has been reported to have 3-4 times more adsorption capacity compared to γ-alumina and used in fluoride removal successfully[22]. It has been reported that activated carbon-alumina composite shows good adsorption capacity towards phenol and potassium dichromate both, whereas only activated alumina could not adsorb phenol and activated carbon could not adsorb potassium dichromate when they are used alone[23].

Therefore, a composite adsorbent material comprising a clay or alumina with activated carbon may be used as an effective adsorbent for the removal of different types of pollutants from waste water. In the present study, alumina-carbon composite (ACC) has been developed and tested for the removal of two different dyes from aqueous solution, namely Methylene Blue (MB) and Alizarin Red-s (ARS). These two dyes are selected on the basis of their different nature, the MB is basic and the ARS is acidic. The effects of different experimental parameters, such as initial dye concentration, *p*H, adsorbent concentration and degree of agitation, on dye adsorption are also studied. The adsorption kinetics and equilibrium study have been done to observe the efficacy of the adsorbent.

*Corresponding author.
E-mail: jkb@che.iitkgp.ernet.in

Experimental Procedure

Materials

Methylene Blue, commercial activated carbon and aluminum nitrate were procured from Merck Specialities Private Limited, Mumbai, India. Alizarin Red-s was supplied by Loba Chemie Pvt. Ltd, Mumbai, India. Alumina was procured from Merck Specialities Pvt. Ltd.

Preparation and characterization of adsorbents

The alumina-carbon composite (ACC) was prepared by *in situ* precipitation of aluminum hydroxide onto commercial activated carbon (CAC) surface. Hundred milliliter of 0.1N aluminum nitrate solution was added into 25 g of activated carbon and then 0.1N ammonia solution was added drop-wise to the mixture under vigorous stirring until the *p*H of the solution reaches to 10. The aluminum hydroxide was precipitated in an amorphous state which is, on further ageing, transformed to bohemite[24]. The reaction is shown below:

$$Al(NO_3)_3 + 3NH_4OH \rightarrow Al(OH)_3\ (s) + 3NH_4NO_3$$

The solid precipitate was washed thoroughly with distilled water, filtered and then dried overnight at 120°C in an air oven. The dried mass was then ground and calcined at 350°C for 3 h. The morphology of the adsorbent was analyzed by SEM and TEM images obtained by scanning electron microscope (Hitachi model SU-70) and transmission electron microscope (Philips Tecnai G2, operating at 180 kV) respectively. The crystalline nature of the adsorbent was examined by the X-ray diffraction image obtained by X-ray diffractometer (Philips PW183). The surface area and pore volume were determined by using BET apparatus (Quantachrome Autosorb-1).

The batch adsorption study

The dye-stock solution (1000 mg/L) was prepared by dissolving the required quantity of dye in distilled water. The equilibrium study was performed by taking different concentration of dye-solution in 500 mL conical flasks with the measured quantities of adsorbent. The kinetic studies were carried out in a stainless steel baffled agitated vessel (diameter 0.112 m and height 0.275 m) placed in a constant temperature water bath. The samples were withdrawn from the vessel at various time intervals. The concentration of MB and ARS in aqueous solution was measured by using UV spectrophotometer (Spectra scan UV 2600, Chemito, India). The adsorption capacity of the adsorbent (q, mg/g) was determined from the mass balance equation and the equilibrium adsorption capacity (q_e) was calculated by the following relationship:

$$q_e = \frac{(C_0 - C_e)V}{m} \quad \ldots (1)$$

where C_e (mg L^{-1}) is the aqueous-phase concentration of dye is in equilibrium; q_e (mg g^{-1}), the surface concentration of the dye; C_0, the initial concentration of the dye solution; V, the volume of solution; and m, the mass of adsorbent.

Sorption isotherms

Five different isotherm models were used to fit the adsorption equilibrium data. The isotherms are:

Freundlich: $q_e = K_1 C_e^n$ ... (2)

Tempkin: $q_e = K_7 log\ (lC_e)$ ... (3)

Langmuir: $q_e = \frac{k_2 q_0 C_e}{1 + k_2 C_e}$ ... (4)

Fritz-Schlünder: $q_e = \frac{k_5 C_e^r}{1 + k_6 C_e^s}$ ... (5)

Redlich-Peterson: $q_e = \frac{k_3 C_e^s}{1 + k_4 C_e^m}$ ... (6)

where q_e is the equilibrium uptake (mg/g); k_2, the Langmuir constant related to the energy of adsorption (L /mg); C_e, the solution concentration at equilibrium (mg/L); q_0, the monolayer adsorption capacity (mg/g); K_1, a rough indicator of the adsorption capacity (L/g); $1/n$, the adsorption intensity; K_7, the equilibrium binding constant which is corresponding to maximum binding energy (L/g); and l(J/mol) corresponds to heat of adsorption.

Kinetic models

The pseudo first- and second-order models[25] were chosen to determine the adsorption dynamics. The pseudo first-order equation is expressed as

$$\log(q_e\text{-}q)=\log q_e - \frac{k_1 t}{2.303} \quad \ldots(7)$$

The pseudo second-order equation is expressed as

$$\frac{t}{q}=\frac{1}{k_2 q_e^2}+\frac{t}{q_e} \quad \ldots(8)$$

where k_1 and k_2 are the pseudo first-order and second - order rate constant respectively.

Results and Discussion

Characterization of ACC

The surface area and average pore size of the adsorbent are found to be 577 m^2/g and 29 Å respectively. The surface area of the alumina prepared separately is 51 m^2/g and pore size is 137 Å. The SEM image of ACC (Fig. 1a) indicates that the alumina particles are approximately 10 nm in size. TEM image (Fig. 1b) shows the uniform distribution of alumina particles on the carbon surface. The EDX analysis of ACC shows that it contains 85.9% of carbon and 14.1% of alumina. The XRD image of ACC given in Fig. 2 confirms **c**rystalline property of the adsorbent.

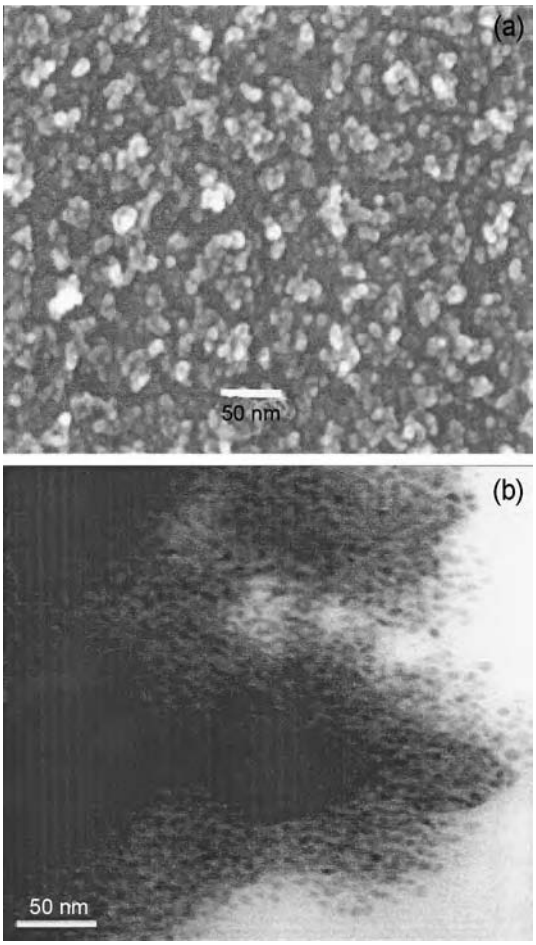

Fig. 1 — (a) SEM image of ACC and (b) TEM image of ACC

Comparison between ACC with CAC

The adsorption capacity of ACC and CAC are compared for both MB and ARS. The ACC shows better adsorption capacity for both MB and ARS (Figs 3a & b). It is observed that, q_e increases as C_e increases, but at high C_e value q_e approaches to a constant maximum value as indicated by the plateau; q_e being maximum adsorption capacity. The adsorption capacity for MB and ARS using ACC are 19.74 and 9.21% greater than the uncoated CAC. The maximum adsorption capacity for MB and ARS are found to be 1152.30 and 522.81 mg/g respectively. The adsorption capacity of ACC for both the dyes is shown to be reasonably high in comparison to other adsorbents as revealed from the previous work[26-33].

Effect of *p*H on adsorption

The adsorption capacity of ACC increases with the *p*H of the solution. It is observed that the adsorption capacity of MB increases from 430 mg/g to 900 mg/g as the solution *p*H increases from 2-8 and the maximum MB removal is obtained at a *p*H of 8. This is due to the basic nature of MB. Similarly, the adsorption capacity of ARS also increases from 106 mg/g to 198.99 mg/g as the solution *p*H increases from 2-5 and the maximum adsorption capacity is achieved at *p*H 5 in case of ARS. The *p*H for ARS is less because of its acidic nature. Therefore, the *p*H of the solution for the subsequent experiments is maintained at 8 for MB and at 5 for ARS.

Effect of stirrer speed

The external mass transfer effect depends on the speed of agitation of the solution by varying the stirrer

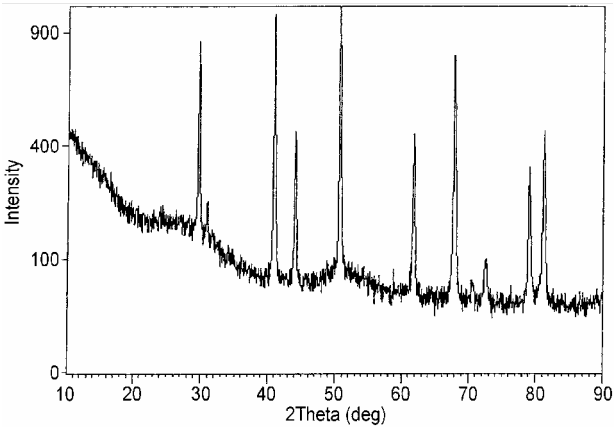

Fig. 2 — XRD image of ACC

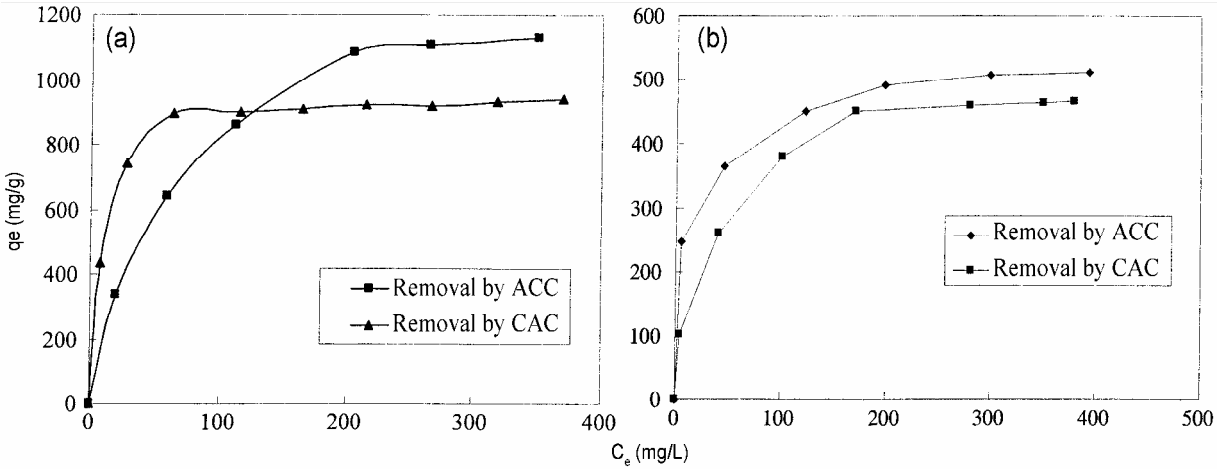

Fig. 3 — Comparison of adsorption capacity of CAC and ACC for (a) MB (temperature 303 K, mass of ACC 0.03 g, volume of solution 100 mL, *p*H 8) and (b) ARS (temperature 303 K, mass of ACC 0.04 g, volume of solution 100 ml, *p*H - 5)

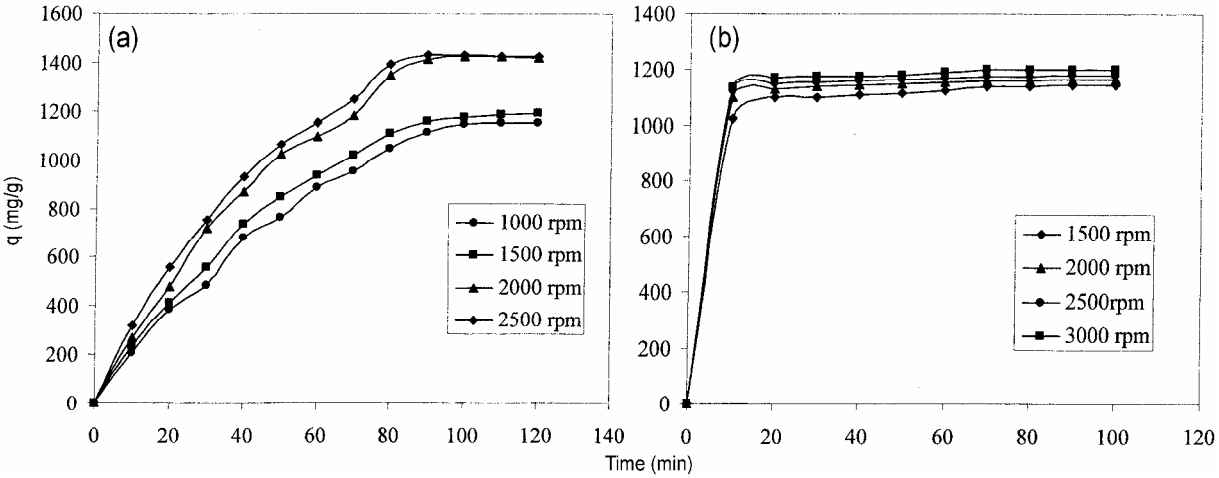

Fig. 4 — Effect of stirrer speed on the removal of (a) MB (temperature 303 K, C_0 - 104.65 ppm, volume of solution 500 mL, mass of ACC 0.03 g, *p*H - 8) and (b) ARS (temperature 303 K, C_0 100 ppm, volume of solution 500 mL, mass of ACC 0.04 g, *p*H-5)

speed. Figures 4a & b show the effects of stirrer speed on the adsorption of MB and ARS respectively. At low stirrer speed, the effect of mass transfer for both the dyes is significant but at higher speed the effect is negligible. As the stirrer speed increases from 1000 rpm to 2000 rpm, the adsorption capacity of ACC increases from 40.78 mg/L to 55.89 mg/L for MB and from 89 mg/L to 94.25 mg/L for ARS in 40 min. It is also noted that the external mass transfer effect is negligible at and above 2000 rpm for both the dyes. So, the subsequent experiments are conducted at 2000 rpm.

Effect of initial concentration

The effects of initial concentrations of MB and ARS on adsorption capacity of the adsorbent are shown in Figs 5a & b. The adsorption capacity shows a steep rise at the initial stage which levels off after acertain period of time. The probable reason for this nature of the curve is that, the initial concentration difference between bulk to the surface of the adsorbent is large which imparts a higher driving force at the beginning of the process. The adsorption capacity increases from 31.02 mg/L to 77.11 mg/L with an increase in initial concentration from 106.87 to 209.79 mg/L for MB. Similarly, the adsorption capacity for ARS increases form 89.45 mg/L to 117.82 mg/L as the initial concentration of ARS increases from 102.1 mg/L to 518.67 mg/L, both the cases the time taken for the measurement of adsorption capacity is 20 min.

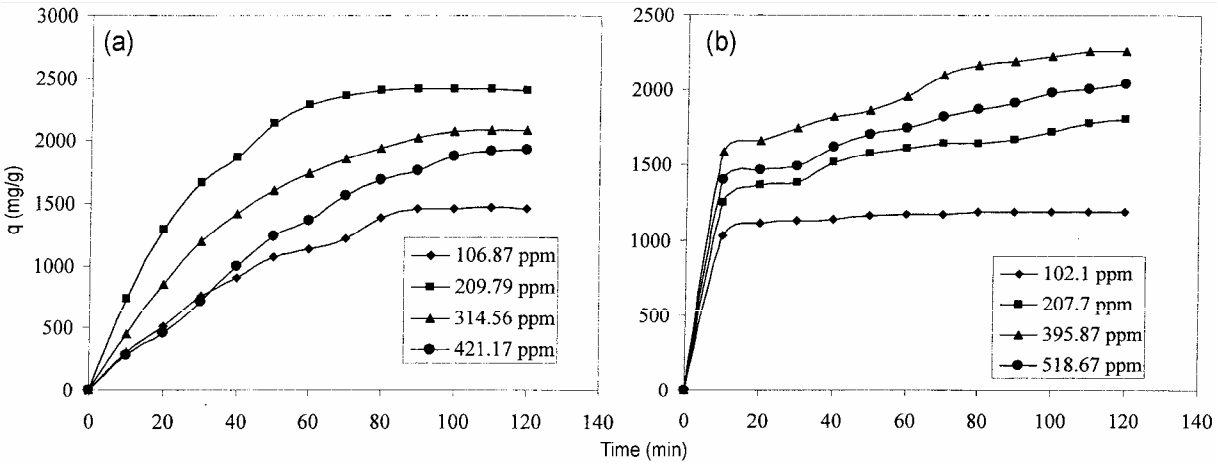

Fig. 5 — Effect of initial dye concentration on the removal of (a) MB (temperature 303 K, mass of ACC 0.03 g, volume of solution 500 mL, stirrer speed 2000 rpm, *p*H-8) and (b) ARS (temperature 303 K, mass of ACC 0.04 g, volume of solution 500 mL, stirrer speed 2000 rpm, *p*H-5)

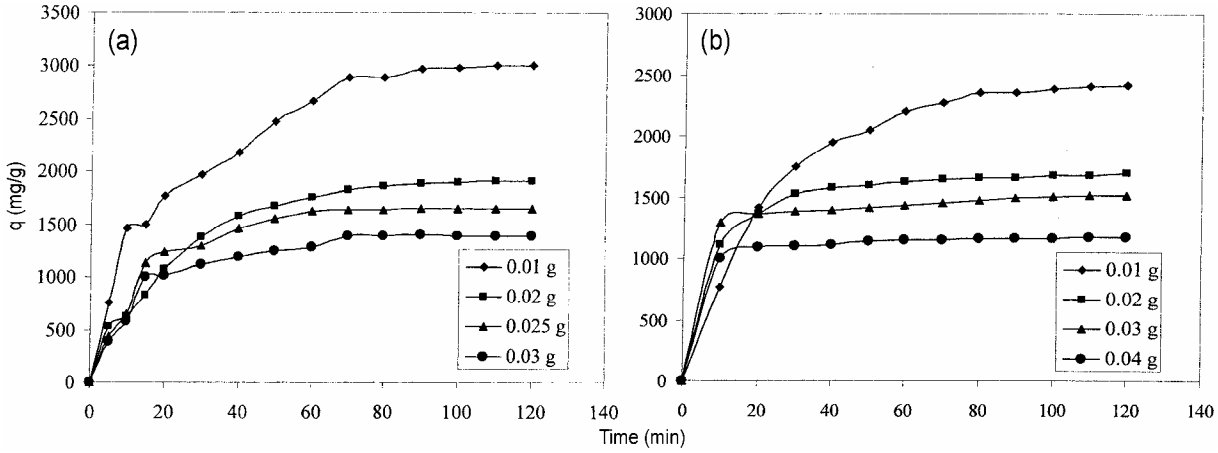

Fig. 6 — Effect of ACC concentration on (a) MB removal (temperature 303 K, C_0- 100 ppm, volume of solution 500 mL, stirrer speed 2000 rpm, *p*H 8) and (b) ARS removal (temperature 303 K, C_0 100 ppm, volume of solution 500 mL, stirrer speed 2000 rpm, *p*H 5)

Effect of adsorbent concentration

The adsorption capacity of ACC increases with increasing its concentration because of the availability of more adsorption sites (Figs 6a & b). It is Observed from the Fig. 6a that the adsorption capacity increases significantly from 35.29 mg/L to 60.65 mg/L after 20 min for MB when ACC concentration increases from 0.01 g to 0.03 g. Similarly, the adsorption capacity for ARS increases from 28.35 mg/L to 87.35 mg/L in 20 min with the increase in ACC concentration from 0.01 g to 0.04 g (Fig. 6b).

Adsorption isotherms

Various adsorption isotherms (e.g. Freundlich, Langmuir, Fritz-Schlunder, Redlich-Peterson and Tempkin) are fitted with the experimental data by nonlinear method of analysis using Matlab 7.1 software. The values of isotherm parameters along with their sum of square error (SSE) for above five isotherms are given in Table 1. The values of SSE indicate that the Redlich-Peterson and Tempkin isotherms show the best fit with the experimental data for MB and ARS respectively.

Kinetic models

The pseudo first-order and pseudo second-order rate expressions have been used to fit the kinetic data. Here, the pseudo first-order rate model [Eq. 7] and second-order rate model(Eq. 8) are fitted well for both MB and ARS. It is observed that the kinetics of adsorption of both the dyes obeys the pseudo second-order rate equation. The values of kinetic parameters for Methylene Blue and Alizarin Red-s are shown in

Table 1— Results of analysis of adsorption isotherm

Isotherm model	Kinetic parameters	
	MB	ARS
Freundlich	K_1=140.975; n=0.368 SSE=272.0	K_1 =199.4349; n=0.164 SSE= 109.0
Langmur	k_2 = 0.015; q_0 = 1372.7 SSE = 3149.6	k_2 = 0.1559; q_0 = 494.65 SSE = 4765.0
Redlich Peterson	k_3 = 18.150; K_4 = 0.008 m = 1.0950; SSE = 2729.8	k_3 = 25.6332; K_4 = 0.038 m = 1.0390; SSE= 18752.0
Fritz schlunder	k_5 = 0.009; K_6 = 0.0001 r =6.504; s =6.1371 SSE =398.6685	k_5 = 0.0354; K_6 = 0.0002 r = 6.392; s = 6.2560 SSE = 27161
Tempkin	K_7 = 295.6875; h = 0.156 SSE = 7321.8	K_7 = 63.7345; h = 1532 SSE = 292.5412

Table 3 — Results of kinetic model analysis of ARS

Rate equation	C_0	Coefficients (95% confidence bounds)	C_r
Pseudo first-order $\log(q_e - q) = a_1 - b_1 t$	102.10	a_1 = -0.02023; b_1 = 1.878	0.936
	207.70	a_1 = -0.01644; b_1 = 2.428	0.741
	395.87	a_1 = -0.01979; b_1 = 2.659	0.839
	518.67	a_1 = -0.0185; b_1 = 2.596	0.795
Pseudo second-order $\frac{t}{q} = a_2 + b_2 t$	102.10	a_2 = 0.004112; b_2 = 0.008589	0.999
	207.70	a_2 = 0.002702; b_2 = 0.02158	0.997
	395.87	a_2 = 0.00205 ; b_2 = 0.02213	0.992
	518.67	a_2 = 0.002319 ; b_2 = 0.02531	0.993

Table 2 — Results of kinetic model analysis of MB

Rate equation	C_0	Coefficients	C_r
Pseudo first-order $\log (q_e - q) = a_1 - b_1 t$	106.87	a_1 = -0.02213 ; b_1 = 2.758	0.730
	209.79	a_1= -0.03094; b_1 = 2.992	0.927
	314.56	a_1 = -0.02406; b_1 = 2.887	0.790
	421.17	a_1 = -0.0237; b_1 = 2.909	0.749
Pseudo second-order $t/q = a_2 + b_2 t$	106.87	a_2 = 0.001812; b_2 = 0.1494	0.983
	209.79	a_2 = 0.001468; b_2 = 0.04787	0.990
	314.56	a_2 = 0.001448; b_2 = 0.08774	0.985
	421.17	a_2 = 0.0008138; b_2 = 0.1731	0.892

Tables 2 & 3 respectively. Pseudo first-order model shows the poor correlation coefficients with negative parameters for all initial dye concentrations and thus it may be rejected.

Conclusion

It has been found that nano-alumina coated activated carbon shows significant amount of adsorption capacities for two different dyes, i.e. Alizarin Red-s and Methylene Blue. The percentage removal of dye increases with the increase in adsorbent dosage and decreases with increase in initial dye concentration. The removal efficiency of an adsorbent increases with increase in *p*H and shows a maximum adsorption for Methylene Blue at *p*H 8 and for Alizarin Red-s at *p*H 5. The adsorption found to increase up to the temperature 30 °C and then shows no further significant increase in uptake above 30°C.

References

1 Gomez V, Larrechi M S & Callao M P, *Chemosphere*, 69 (2007) 1151.
2 Gonga R, Lic M, Yang C, Suna Y & Chenb J, *J Hazard Mater,* B121 (2005)247.
3 Bishnoi N R, Bajaj M, Sharma N & Gupta A, *Biores Technol*, 91 (2004)305.
4 Malkoc E & Nuhoglu Y, *Sep Purif Technol*, 54 (2007) 291.
5 Iqbal M J & Ashiq MN, *J Hazard Mater*, B139 (2007) 57.
6 Ong S T, Lee C K & Zainal Z, *Biores Technol*, 98 (2007) 2792.
7 Ying W, Kongjun Z, Fen W & Kazumichi Y, *J Environ Sci,* 2 (2009) 434.
8 Vipasiri V, Lei J B, Chowd C W K & Saint C, *Chem Eng J*, 148 (2009) 354.
9 Gürses A, Karaca S, Dogar Ç, Bayrak R, Açıkyıldız M & Yalçın M, *J Colloid Interf Sci*, 269 (2004) 310.
10 Alkan M, Demirbas O & Dogan M, *Microporous Mesoporous Mat*,101 (2007) 388.
11 Karagozoglu B, Tasdemir M, Demirbas E & Kobya M, *J Hazard Mater*, 147 (2007) 297.
12 Santos S C R & Boaventura R A R, *Appl Clay Sci*, 42 (2008) 137.
13 Eren E, Cubuk O, Ciftci H, Eren B & Caglar B, *Desalination*, 252 (2010) 88.
14 Kannan C, Sundaram T & Palvannan T, *J Hazard Mater*, 157 (2008) 137.
15 Adak A, Bandyopadhyay M & Pal A, *Sep Purif Technol*, 44 (2005) 39.
16 Venkata M S & Karthikeyan, *J Environ Pollut*, 97 (1,2) (1997) 183.
17 Onganer Y & Temur C, *J Coll Interf Sci*, 205 (1998) 241.
18 Morais L C, Freitas O M, Gongcalves E P , Vasconcelos L T & Gonzaalez Beca C G, *Water Res*, 33 (4) (1999) 979.
19 Malik P K, *J Hazard Mat*er, B113 (2004) 81.
20 Rodr´ıguez-Reinoso F, Molina-Sabio M & Gonza´lez J C, *Carbon*, 39 (2001) 771.
21 Hussein M Z B, Kuang D, Zainal Z & Teck T K, *J Colloid Interf Sci*, 235 (2001) 93.
22 Wang S, Li Y, Zhao D, Xu C, Luan Z, Liang J & Wu D, *Chinese Sci Bull*, 47 (9) (2002) 722.
23 *Activated carbon alumina composite, U S Pat*, 4,795, 735, (1989).
24 Moscou L & Van der Vlies G S, *Colloid Polym Sci*, 163 (1) (1959) 35.
25 Igwe J C, Mbonu O F & Abia A A, *J Appl Sci*, 7 (2007) 2840-2847.
26 Hameed B H, *J Hazard Mater*, 162 (2-3) (2009) 939-944.
27 Hameed B H, Mahmoud D K & Ahmad A L, *Colloids Surf A: Physicochem Eng Aspects*, 316 (78-84) (2008).
28 Hameed B H & Daud F B M, *Chem Eng J*, 139 (2008)(1), 48-55.
29 Karagöz S, Tay T, Ucar S & Erdem M, *Bioresour Technol*, 99 (14) (2008) 6214–6222.
30 Hameed B H, Din A T M & Ahmad A L, *J Hazard Mater,* 141 (3) (2007) 819–825.
31 Hameed B H, Ahmad A L & Latiff K N A, *Dyes Pigm*, 75 (1) (2007) 143–149.
32 Ahmad A L, Loha M M & Aziz J A, *Dyes Pigm*, 75 (2) (2007) 263–272.
33 Iqbal M J & Ashiq M N, *J Hazard Mater*, 139(1) (2007) 57-66.